

See discussions, stats, and author profiles for this publication at: <https://www.researchgate.net/publication/5684304>

The PsaE subunit of photosystem I prevents light-induced formation of reduced oxygen species in the cyanobacterium *Synechocystis* sp. PCC 6803

ARTICLE in *BIOCHIMICA ET BIOPHYSICA ACTA* · APRIL 2008

Impact Factor: 4.66 · DOI: 10.1016/j.bbapbio.2007.11.009 · Source: PubMed

CITATIONS

17

READS

30

4 AUTHORS, INCLUDING:



Robert Jeanjean

71 PUBLICATIONS 1,253 CITATIONS

SEE PROFILE



Amel Latifi

Aix-Marseille Université

42 PUBLICATIONS 2,312 CITATIONS

SEE PROFILE



Hans C P Matthijs

University of Amsterdam

156 PUBLICATIONS 2,409 CITATIONS

SEE PROFILE

The PsaE subunit of photosystem I prevents light-induced formation of reduced oxygen species in the cyanobacterium *Synechocystis* sp. PCC 6803

Robert Jeanjean^a, Amel Latifi^a, Hans C.P. Matthijs^b, Michel Havaux^{c,*}

^a Laboratoire de Chimie Bactérienne, CNRS-UPR 9043, Institut de Biologie Structurale et Microbiologie,
31 chemin Joseph Aiguier, F-13402 Marseille cedex 20, France

^b University of Amsterdam, Institute for Biodiversity and Ecosystem Dynamics, NL-1018WS Amsterdam, The Netherlands

^c CEA/Cadarache, iBEB, SBVME, Laboratoire d'Ecophysiologie Moléculaire des Plantes,
UMR 6191 CNRS-CEA-Université Aix Marseille, F-13108 Saint-Paul-lez-Durance, France

Received 8 November 2007; received in revised form 28 November 2007; accepted 28 November 2007

Available online 5 December 2007

Abstract

The PsaE protein is located at the reducing side of photosystem I (PSI) and is involved in docking the soluble electron acceptors, particularly ferredoxin. However, deletion of the *psaE* gene in the cyanobacterium *Synechocystis* sp. strain PCC 6803 inhibited neither photoautotrophic growth, nor *in vivo* linear and cyclic electron flows. Using photoacoustic spectroscopy, we detected an oxygen-dependent, PSI-mediated energy storage activity in the *ΔpsaE* null mutant, which was not present in the wild type (WT). The expression of the genes encoding catalase (*katG*) and iron superoxide dismutase (*sodB*) was upregulated in the *ΔpsaE* mutant, and the increase in *katG* expression was correlated with an increase in catalase activity of the cells. When catalases were inhibited by sodium azide, the production of reactive oxygen species was enhanced in *ΔpsaE* relative to WT. Moreover, sodium azide strongly impaired photoautotrophic growth of the *ΔpsaE* mutant cells while WT was much less sensitive to this inhibitor. The *katG* gene was deleted in the *ΔpsaE* mutant, and the resulting double mutant was more photosensitive than the single mutants, showing cell bleaching and lipid peroxidation in high light. Our results show that the presence of the PsaE polypeptide at the reducing side of PSI has a function in avoidance of electron leakage to oxygen in the light (Mehler reaction) and the resulting formation of toxic oxygen species. PsaE-deficient *Synechocystis* cells can counteract the chronic photoreduction of oxygen by increasing their capacity to detoxify reactive oxygen species.

© 2007 Elsevier B.V. All rights reserved.

Keywords: Photosystem; Photooxidative stress; Oxygen photoreduction; Catalase; Lipid peroxidation; Cyanobacteria

1. Introduction

In photosynthetic organisms, the concerted action of photosystem II and photosystem I (PSII and PSI) in linear photosynthetic electron flow produces NADPH and ATP according to the Z-scheme, and there is a large consensus about the role of the photosystems and the electron carriers involved in this pathway [1–3]. A balanced photosynthetic electron flow needs a tight continuity between membrane-embedded electron carriers

Abbreviations: PS, photosystem; FNR, Ferredoxin:NADP⁺ oxidoreductase; PFD, photon flux density; OD, optical density; P700, PSI reaction center pigment; ES, energy storage; ROS, reactive oxygen species; WT, wild type; SOD, superoxide dismutase; PTOX, plastid terminal oxidase

* Corresponding author. Fax: +33 4 4225 6265.

E-mail address: michel.havaux@cea.fr (M. Havaux).

0005-2728/\$ - see front matter © 2007 Elsevier B.V. All rights reserved.

doi:10.1016/j.bbabio.2007.11.009

and soluble carriers. For instance, electron transfer to ferredoxin at the stromal side of PSI is favored by the docking of ferredoxin to PSI subunits, as was concluded from cross-linking experiments [4,5] and from evidence for the role of the PsaE subunit in ferredoxin or flavodoxin binding to PSI [6–10]. Together with PsaC and PsaD, PsaE is a stromal extrinsic PSI subunit that does not contain cofactors [11]. While PsaC is essential for electron transport via the binding of the terminal electron acceptors F_A and F_B [12], PsaD and PsaE are thought to be involved in ferredoxin binding [13,14]. Additionally, PsaD is required for the assembly of PsaC and PsaE into the PSI complex. The PsaC–E subunits are located at a crucial branchpoint of PSI-mediated electron transport where electrons can be dispatched into the linear, cyclic and pseudocyclic electron pathways. The pseudocyclic electron transport involves oxygen as terminal electron

acceptor and is thus associated with generation of reduced forms of oxygen, including highly toxic ones with potential to cause oxidative stress [15].

Deletion of the *psaE* gene in the cyanobacterium *Synechocystis* increased the dissociation rate of the PSI/ferredoxin complex, suggesting that PsaE controls the lifetime of this complex [9]. The *psaE* mutation also introduces lowered rates of ferredoxin and NADP⁺ photoreduction as measured by in vitro assays [7,8,16]. However, raising the concentration of ferredoxin allowed PsaE-deficient PSI complexes to reach similar photoreduction rate as the WT complexes [9]. Van Thor et al. [16] assumed that a ternary complex PSI–ferredoxin–ferredoxin: NADP⁺ oxidoreductase (FNR) takes place in the WT, which is mediated by the PsaE protein, and they showed using in vitro assays that the PSI–NADP⁺ photoreduction rate at high FNR concentrations in the *ΔpsaE* mutant is close to the WT reduction rate. This suggests that the loss of affinity of PSI for the different carriers in the absence of PsaE could be partially compensated by increasing the FNR concentration. Consistently, *Synechocystis* cells responded to *psaE* gene deletion by increasing the amount of FNR transcripts and proteins [16]. This may establish cellular conditions allowing electron transfer reaction rates and photosynthetic activity close to the WT level and can explain why *ΔpsaE* mutants of *Synechococcus* and *Synechocystis* are able to grow under photoautotrophic conditions with rates comparable to WT [8,17]. However, PsaE-mediated binding of ferredoxin and FNR to PSI as a ternary complex has been recently criticized by Cassan et al. [18] based on in vitro measurements of reoxidation kinetics of reduced ferredoxin using flash-absorption spectroscopy. Alternatively, it has been suggested, based on P700 turnover measurements in *Synechococcus*, that the PsaE protein could be involved in cyclic electron flow around PSI [13,19]. However, this hypothesis was questioned in subsequent studies by Charlebois and Mauzerall [20] and Thomas et al. [21] who observed no significant difference in PSI cyclic activity between WT and *ΔpsaE* mutant cells of *Synechococcus* or *Synechocystis*. Because of those contradictory results, the exact function of PsaE in cyanobacteria is still elusive. Moreover, the possible regulatory role of the stromal extrinsic subunits of PSI, PsaD and PsaE, in electron transfer to oxygen has never been investigated.

Disruption of the *psaE* genes has also been performed in the vascular plant *Arabidopsis thaliana* [22,23]. Although PsaE-deficient *Arabidopsis* mutants were able to grow photoautotrophically, they were greatly impaired in photosynthetic electron flow, in growth rate, in leaf coloration, and they bleached during exposure to high light. Such discrepancy between the growth capacities of the cyanobacterial mutants and the plant mutants raises questions about the requirement of the PsaE subunit in photosynthesis.

In this study, we have reconsidered the involvement of PsaE in the cycling of electrons around PSI. The cyclic electron activity was measured in a *ΔpsaE* null mutant of *Synechocystis* sp. strain PCC 6803 using photoacoustic spectroscopy and kinetic spectrophotometry under different gas conditions. This study includes also a double mutant deleted in *psaE* and *ndhB*. Our results demonstrate that suppression of the PsaE subunit does not inhibit cyclic electron transport activity of PSI.

Instead, we found an oxygen-dependent energy storage activity that was not displayed by WT. The presented results support the idea that this additional activity is oxygen photoreduction by the Mehler reaction, suggesting a new physiological role for PsaE in cyanobacteria.

2. Materials and methods

2.1. Material, culture conditions and treatments

Synechocystis sp. strain PCC 6803 was grown at 34 °C in modified Allen's medium (12 mM NaHCO₃) [24], when WT was grown in parallel with the *ΔndhB* and *ΔndhB/ΔpsaE* mutants, or in BG11 medium at a photon flux density (PFD) of about 40 μmol photons m⁻² s⁻¹ on a rotary shaker (170 rpm), as in [25]. High light stress was imposed by transferring cell suspensions to a PFD of 500 μmol m⁻² s⁻¹ for 18 h. Cell growth was monitored by measuring the optical density (OD) of the cell suspensions at 750 nm.

2.2. Genetic constructions

The plasmid pFBsKE2 was provided by Dr. B. Lagoutte (CEA/Saclay, France). This plasmid is deleted of the *psaE* gene and contains the flanking region of the gene which was replaced by a kanamycin resistance (Kmr) cassette from transposon Tn903 (Pharmacia) [7]. The kanamycin resistance was removed after digestion by PstI and replaced with a streptomycin/spectinomycin resistance cassette. The resulting plasmid pFBSA was used to transform the WT and the *ΔndhB* mutant (M55). The transformants were selected by their resistance to streptomycin. Full segregation of the mutants was checked by PCR.

The construction of the mutant *katGi* was identical to that reported in [26]. The gene *katG* was amplified by PCR (Expand, Roche) with the following primers (5' KatGisyNotI: ATAAGAAT GCG GCC GC ACC ATC GTA AGG AAA AAC CCA, 3' KatGisyE: CCG GAATTC TTG CTG AAA TGT TGC CTG AAT), digested by NotI and EcoRI and ligated with the plasmid Blue Script. The cloned fragment was digested by HpaI and ligated with the kanamycin resistance gene released by a digestion HincII from the plasmid puc4K. The derived plasmid KatGiKm was used to transform our glucose-tolerant *Synechocystis* PCC 6803 strain. The transformants bearing the kanamycin resistance were checked by PCR (primers 5NkatGVer: GGC TTG CTT CCA GTG ACC ATC, 3katver TCC TGG GGC ACA TCG GGG C), which allowed to identify a fully segregated interruption mutant (*katGi*). The double mutant *ΔpsaE–katGi* was selected by transformation of the *ΔpsaE* mutant with the DNA extracted from the mutant *katGi*. The complete segregation of the double mutant was also checked by PCR. The deletion of the *psaE* gene was checked with the primers used formerly for cloning by Rousseau et al. [7].

2.3. Photoacoustic measurements

Energy storage in far-red light was measured *in vivo* using the photoacoustic technique, as described in detail elsewhere [27,28]. The cyanobacterial suspension (40 μg) was filtered under pressure through a MF Millipore filter of 1.2 cm diameter (mixed ester cellulose nitrate/acetate, 3 μm pore size). The filter with an evenly distributed layer of cyanobacteria was placed in the photoacoustic cell of laboratory-built photoacoustic spectrometer [28]. Photoacoustic measurements under nitrogen atmosphere were done by flushing nitrogen in the cell for about 60 s and rapidly closing the cell. The samples were illuminated with light filtered through a RG715 filter (Schott) to provide PSI-light and modulated at 16 Hz. The fluence rate of the resulting far-red light was adjusted with neutral density filters (Schott). Photochemistry was saturated by a strong non-modulated white light (ca. 900 W m⁻²). Energy storage was calculated as the difference between the maximal (light-saturated) photothermal signal and the actual signal with far-red light only, and normalized to the maximal signal [27].

2.4. P700 redox state measurements

Changes in the redox state of the reaction center P700 of PSI were monitored via cell absorbance changes at around 820 nm [29], using a modulated fluorescence measurement system MKII (P700⁺ accessory kit) from Hansatech

(Hansatech Instrument Ltd) coupled to a computer. The reaction center P700 of the cyanobacterial sample (20 to 40 μg Chl), which were deposited on a Millipore membrane placed in the leafclip system from Hansatech, was oxidized by illumination with far-red light (730 nm, 8 W m^{-2}) supplied by a LS2 lamp (100 W tungsten–halogen light source, Hansatech) and an interference filter (730FS10, Corion). The kinetics of the P700⁺ reduction in the dark after interrupting the far-red light were recorded. The half-time of the P700⁺ reduction in the dark was used as a measure of the turnover of the P700 reaction center in the cyclic electron transport pathway [30].

2.5. RNA manipulations (RT-PCR)

Harvested cells were treated by RLT+ mercaptoethanol buffer (Qiagen). After several phenol–chloroform extractions, total RNA was loaded on RNA easy column (Qiagen), followed by DNase treatment (RNase free DNase, Qiagen). After elution and estimation of RNA (at 260 nm), the absence of DNA was checked by routine PCR and then RT-PCR was carried out as in Ardelean et al. [25] with the Superscript one-step RT-PCR kit from Invitrogen. Semi-quantitative RT-PCR was performed in order to estimate the amounts of transcript of *sodB* (*slr1516*), *katG* (*sll1987*), *ahpC* (*sll1621*) and *rnpA* (*slr1469*) with the following primers:

sodB: 5' primer GACTACACCGCTCTGGAACCC, 3' primer AACACCAACCAAGCCAGCCG
KatG: 5' primer GCC CCG ATG TGC CCC AGG AA, 3' primer ATC GCC GCT CCC CCT CCT A
ahpC: 5' primer GGT TGT GCT TTT CTC CCT AC, 3' primer CAC CGA ACT CAG GCT CAA TAA
rnpA: 5' primer GCAAGATTTCAGACCGTTTA, 3' primer TGGCTA AATACTGCTCTAAT

2.6. Oxygen exchange and determination of catalase activity

According to [26], the catalase activity in *Synechocystis* is strongly dependent of the growth phase. For this reason the experiments were done when cells of WT and mutants reached the same cell density. Cells were harvested by centrifugation, rinsed, and suspended in 50 mM HEPES–NaOH (pH 7.5), 0.8 M sorbitol, 1 mM benzamidine and 1 mM phenylmethylsulfonyl fluoride at 4 °C. Cells were subsequently broken by shaking with glass beads in a cooled Vibrogen-Zellmühle (E. Bühler). Aliquots of the supernatant of cell homogenates, resulting from two successive centrifugations that eliminate the cell debris at 5000 g, were diluted in a potassium phosphate buffer (25 mM, pH 8) as described in [31]. The catalase activity was followed by the decrease of absorbance at 240 nm by means of an Uvikon 930 spectrophotometer using a $\Delta\epsilon$ of $35 \text{ mM}^{-1} \text{ cm}$ at room temperature. The oxygen exchange was measured on whole cells suspended in growth medium (about 3 to 4 μg Chl) with an oxygen electrode (Rank Bros.). The release of oxygen after adding hydrogen peroxide (5 mM) was recorded under dark conditions.

2.7. Estimation of ROS formation in the light

The quantification of ROS formation during illumination was done as in [32] with a spectrofluorimeter (SAFAS) by using the fluorescent probe 5-(and-6)-chloromethyl-2,7-dichlorodihydrodihydrofluorescein diacetate, acetyl ester (CM-H₂DCFH-DA, Molecular Probes, Invitrogen, C6827) at a final concentration of 25 μM . Fluorescence was excited at 488 nm and detected at 525 nm. The fluorescent probe detects hydrogen peroxide, hydroxyl radical and peroxy radical anions.

2.8. Autoluminescence imaging

Cell suspensions were adapted for 2 h to darkness before recording spontaneous photon emission. Photon emission was recorded at room temperature with a nitrogen-cooled CCD camera as previously described [33]. Integration time was 60 min.

3. Results

3.1. Cyclic electron transport around PSI

Cyanobacterial cells deposited on a filter were irradiated with modulated far-red light in a small photoacoustic chamber. The pulsed heat emission generates an acoustic signal within the chamber, which can be measured by a sensitive microphone, and Fig. 1A shows a representative photoacoustic signal emitted by WT and *ApsaE* mutant cells. Saturation of the photochemical activity by addition of a strong non-modulated light to the modulated light beam increased thermal energy dissipation and produced a rise in the photoacoustic signal. The difference between the maximal heat emission thus obtained and the actual level of the photoacoustic photothermal level corresponds to the fraction of absorbed far-red light energy that was stored into photochemical products [34]. When the photoacoustic

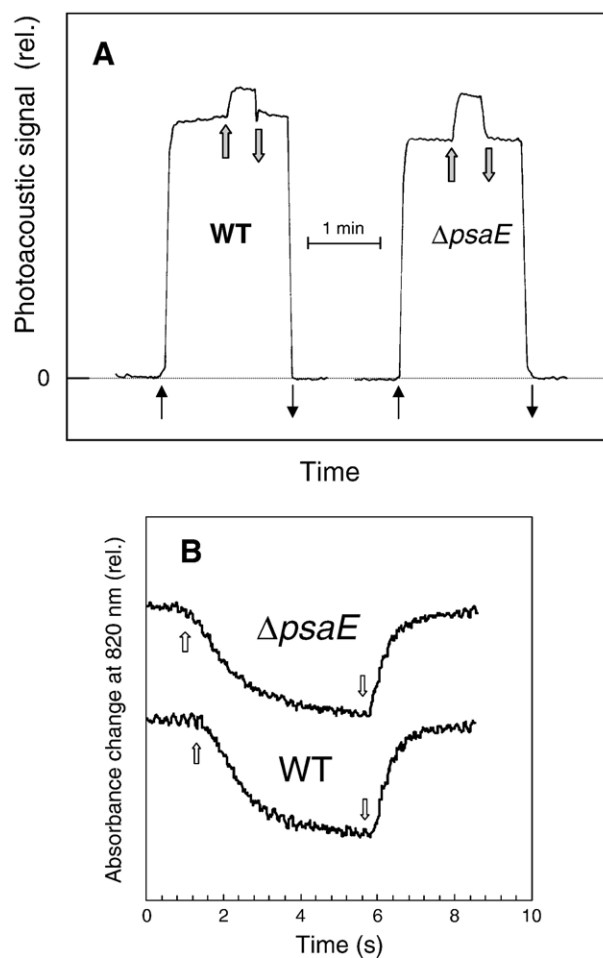


Fig. 1. Cyclic electron flow around PSI in WT cells of *Synechocystis* sp. strain PCC 6803 and in *ApsaE* mutant cells. A) Photoacoustic signals generated by filter-deposited WT and *ApsaE* cells. The wavelength of the measuring light was specific for PSI ($>715 \text{ nm}$, 15 W m^{-2}). The thin (black) upward- and downward-pointing arrows indicate that the modulated far-red light was switched on and off, respectively. The grey upward- and downward-pointing arrows indicate that saturating continuous light was switched on and off, respectively. B) Changes in the redox state of P700 were monitored in whole cells via absorbance changes around 820 nm. The upward- and downward-pointing arrows indicate that far-red light (730 nm , 6 W m^{-2}) was switched on and off, respectively.

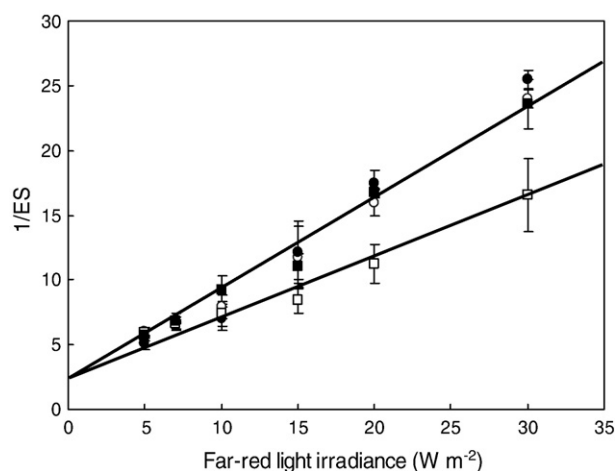


Fig. 2. Dependence of the reciprocal of photochemical energy storage ($1/ES$) on the modulated far-red light irradiance in WT and *ApsaE* *Synechocystis* cells under aerobic and anaerobic conditions. Anaerobiosis was achieved by flushing gaseous nitrogen in the photoacoustic cell. Open squares, *ApsaE* under aerobic conditions; Closed squares, *ApsaE* under anaerobic conditions; Open circle, WT under aerobic conditions; Closed circles, WT under anaerobic conditions. Data are mean values of 3 separate experiments \pm SD.

experiments are performed in far-red light absorbed almost exclusively by PSI, the measured energy storage (ES) is related to the PSI photochemical activity, mainly cyclic electron transport [27,34]. ES by *ApsaE* mutant cells appeared to be increased compared to ES by WT cells. We also measured the re-reduction of oxidized P700 after a transition from far-red light to darkness using kinetic spectrophotometry at 820 nm. This indicates the rate of electron donation from the stroma to the P700 reaction center [30]. The kinetics of P700 reduction did not show any significant difference between WT and the *ApsaE* mutant (Fig. 1B). Thus, the capacity of cyclic electron transport around PSI in far-red light does not seem to be inhibited in the *ApsaE* mutant. The experiments of Charlebois and Mauzerall [20] carried out on the *ApsaE* mutant of *Synechococcus* led to a similar conclusion.

The plot of the reciprocal of ES versus the far-red light irradiance is linear [28,35]. The plots shown in Fig. 2 confirmed that ES was substantially increased (or $1/E$ was substantially decreased) in the *ApsaE* mutant relative to WT, particularly at high light irradiances. However, this increase was cancelled when oxygen was removed from the photoacoustic cell by flushing gaseous nitrogen. This effect is summarized in Table 1. Compared

to WT, ES was increased by 50% in *ApsaE* in air, but not in nitrogen. In contrast, the postillumination P700⁺ reduction rate was similar in WT and *ApsaE* in both gas conditions. In anaerobic conditions, we observed a substantial increase in the P700 reduction half-time relative to aerobic conditions, and this could be due to an over-reduction of the electron transfer chain and the failure of the redox poise control. It is known that optimal electron transport requires accurate redox poisoning of the cyclic system [36], and it is likely that over-reduction of the intersystem electron transport chain hampered electron flow through cytochrome *b6/f*. One can conclude from the stimulatory effect of oxygen on ES that, in the *ApsaE* mutant, an oxygen-dependent, energy-storing reaction occurs in far-red light in addition of the normal PSI cyclic activity. We speculate that this reaction is oxygen photoreduction at the PSI stromal side through the Mehler reaction.

As shown previously [16,37], cyclic electron transport around PSI, as monitored by ES and dark P700 reduction, was strongly inhibited in a *AndhB* mutant lacking a functional NDH-1 complex (Table 1). The remaining cyclic activity is attributable to the antimycin-sensitive pathway [38]. We generated a double mutant *ApsaE/AndhB* deficient in both NDH-1 and PsaE. Removing PsaE from the *AndhB* mutant had the same effect on ES than that observed in WT. As for the single mutant, ES was stimulated in the absence of PsaE, and this stimulation was suppressed by flushing nitrogen in the photoacoustic chamber. It is clear from these results that, contrary to a previous suggestion [19], PsaE is not involved in the NDH1-independent cyclic electron pathway. Rather, lack of PsaE induced, both in WT cells and *AndhB* cells, an additional electron transfer activity relying on the presence of oxygen.

3.2. ROS-scavenging capacity

Donation of electrons from PSI to oxygen produces ROS, such as superoxide and hydrogen peroxide, which are hazardous for many biological processes [15,39]. Therefore, induction of oxygen photoreduction in the *ApsaE* mutant should promote ROS production in the light and photooxidative damage. However, the *ApsaE* mutant did not present any kind of strong deficiencies compared to WT, and it grew very well under regular conditions. The *psaE* mutation had no effect on cell growth at 40 $\mu\text{mol photons m}^{-2} \text{s}^{-1}$ (Fig. 3A) or at a moderately elevated PFD of 200 $\mu\text{mol m}^{-2} \text{s}^{-1}$ (data not shown). Therefore, it is possible that the mutant up-regulated its ROS-scavenging activity to cope with the increased ROS production associated

Table 1

Energy storage ES (in % of absorbed light) and P700 reduction half-time $t_{1/2}$ (in ms) in WT, *ApsaE* mutant, *AndhB* mutant and double mutant *AndhB/ApsaE* illuminated with far-red light under aerobic and anaerobic conditions

	WT		<i>ApsaE</i>		<i>AndhB</i>	<i>AndhB/ApsaE</i>	
	Aerobic conditions	Anaerobic conditions	Aerobic conditions	Anaerobic conditions	Aerobic conditions	Aerobic conditions	Anaerobic conditions
ES	7.6 \pm 0.7	8 \pm 0.8	12 \pm 1.4	7.8 \pm 0.9	2.8 \pm 0.5	5.2 \pm 1	3.2 \pm 0.2
(%)	(4)	(3)	(3)	(3)	(5)	(4)	(3)
$t_{1/2}$	280 \pm 40	450 \pm 50	290 \pm 30	430 \pm 50	1400 \pm 140	1600 \pm 80	N.D.
(Ms)	(8)	(3)	(6)	(4)	(4)	(4)	

For the photoacoustic measurements of ES, the far-red light irradiance was 15 W m^{-2} . The dark reduction of oxidized P700 was measured after illumination with far-red light of 6 W m^{-2} . Anaerobiosis was reached after 10 min in the presence of glucose (20 mM) and glucose oxidase and flushing nitrogen gas in the photoacoustic cell. N.D. = not determined. Data are mean values \pm standard deviation. In parentheses, number of repetitions.

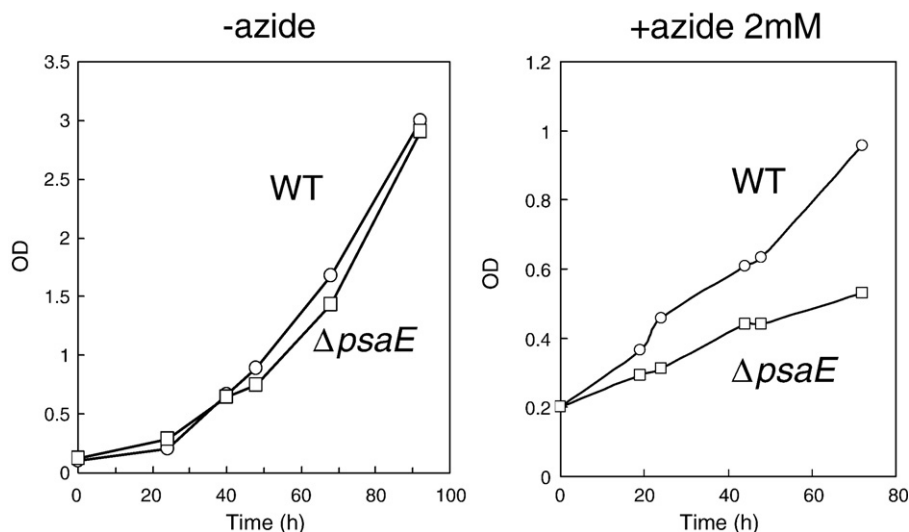


Fig. 3. Growth curves of WT *Synechocystis* PCC6803 and the $\Delta psae$ mutant in BG-11 medium containing 0 or 2 mM sodium azide (A and B, respectively). PFD was $50 \mu\text{mol photons m}^{-2} \text{s}^{-1}$. Cell densities were estimated from measurements of the optical density (OD) of cell suspension at 750 nm. These experiments were repeated 3 times with qualitatively similar results.

with oxygen photoreduction. Accordingly, when cells were grown in the presence of sodium azide, a potent inhibitor of catalases [40], growth of $\Delta psae$ was substantially more impaired than that of WT (Fig. 3B). This differential sensitivity of WT and $\Delta psae$ to azide prompted us to examine the catalase activity in both strains (Fig. 4). Oxygen release by $\Delta psae$ mutant cells incubated with hydrogen peroxide in the dark was about 30% higher than in WT. This result was also obtained when the rate of hydrogen peroxide decomposition was studied in cell homogenates: the catalase activity (in $\mu\text{mol H}_2\text{O}_2$ decomposed per min and per mg proteins) was similar in WT and the $\Delta andhB$ mutants (6.6 ± 0.1 and 6.0 ± 1.0 , respectively) and was substantially increased in the $\Delta psae$ and $\Delta psae/\Delta andhB$ mutants (8.5 ± 0.1 and 9.0 ± 1.0 , respectively). As expected, the activity was sensitive to sodium azide in both strains (Fig. 4). The increased activity of catalase in $\Delta psae$ was correlated with an increase in the transcript level of the *katG* gene encoding catalase (Fig. 5B). Similarly, the *sodB* gene encoding iron superoxide dismutase (SOD) was upregulated in the $\Delta psae$ mutant (Fig. 5B).

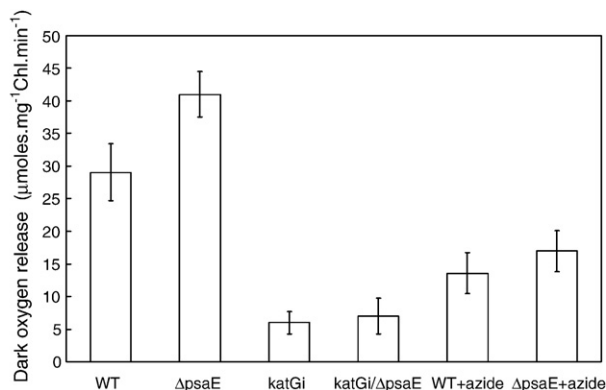
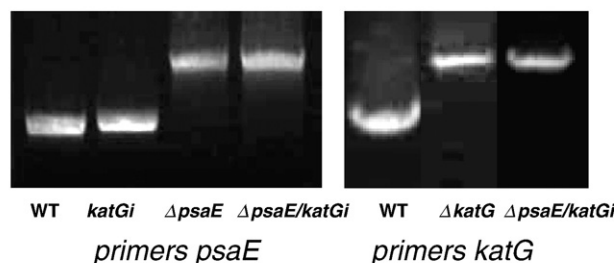


Fig. 4. Oxygen release by WT, $\Delta psae$, *katGi* and $\Delta psae$ –*katGi* cells after adding 5 mM H_2O_2 in the dark. The effects of 2 mM sodium azide was examined in WT and $\Delta psae$. Data are mean values of 4 separate experiments \pm SD.

3.3. ROS production in the light

The formation of ROS during illumination with white light of $500 \mu\text{mol photons m}^{-2} \text{s}^{-1}$ was monitored with the fluorescent probe CM- $\text{H}_2\text{DCFH-DA}$, as previously described [32,41]. This ROS reporter dye diffuses passively into the cells and fluoresces

A : PCR



B : RT-PCR

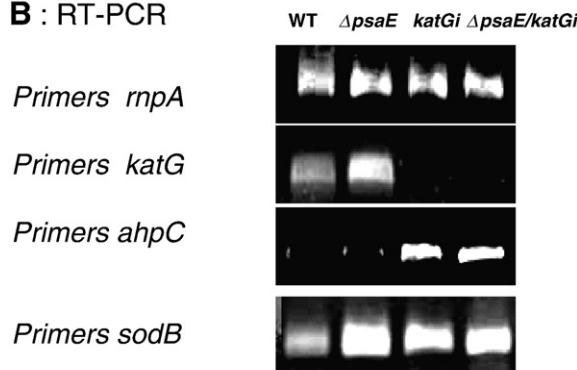


Fig. 5. PCR and RT-PCR carried out on DNA and total RNA. A) PCR carried out on DNA from WT, $\Delta psae$, *katGi* and $\Delta psae$ –*katGi* with the primers *psaE* and *KatG*. B) Level of transcription of the *katGi*, *sodB* and *ahpC* genes in WT *Synechocystis* and the $\Delta psae$, *katGi* and $\Delta psae$ –*katGi* mutants determined by semi-quantitative RT-PCR. The *rnpA* gene (encoding a subunit of the ribonuclease P) was used as internal control of equal RNA loading.

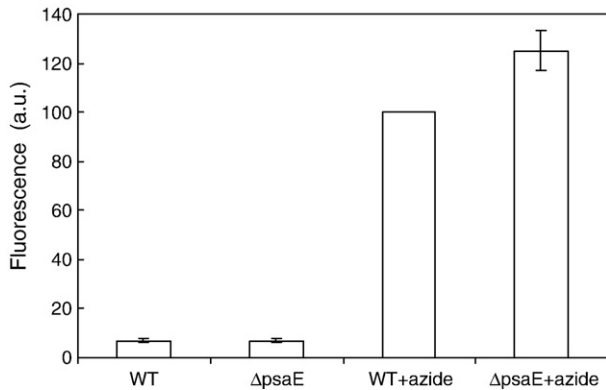


Fig. 6. Detection of photooxidative stress in WT and $\Delta psaE$ mutant cells of *Synechocystis* sp. PCC 6803. Light-induced production of ROS was measured by the fluorescence intensity of CM- $H_2DCFH-DA$. Cells ($10 \mu g$ Chl/ml) were incubated with the fluorescent probe ($25 \mu M$ final concentration) and exposed to high light ($500 \mu mol m^{-2} s^{-1}$) for 20 min, without or with 1 mM sodium azide. Fluorescence at 525 nm was excited with a light beam at 488 nm. Data are mean values of 4 separate experiments. Because the intensity of the fluorescence signal in azide-treated cells varied from one experiment to the other, we normalized the signal of WT in the presence of azide to 100, and we calculated the SD for the fluorescence values measured in the $\Delta psaE$ mutant.

brightly when oxidized. ROS-induced fluorescence was similar in WT and the $\Delta psaE$ mutant (Fig. 6). When the same experiment was done in the presence of 1 mM azide, ROS production was strongly increased ($\times 10$), as expected if catalase is inhibited. Interestingly, under these conditions, the ROS-induced fluorescence in $\Delta psaE$ cells was significantly higher than that measured

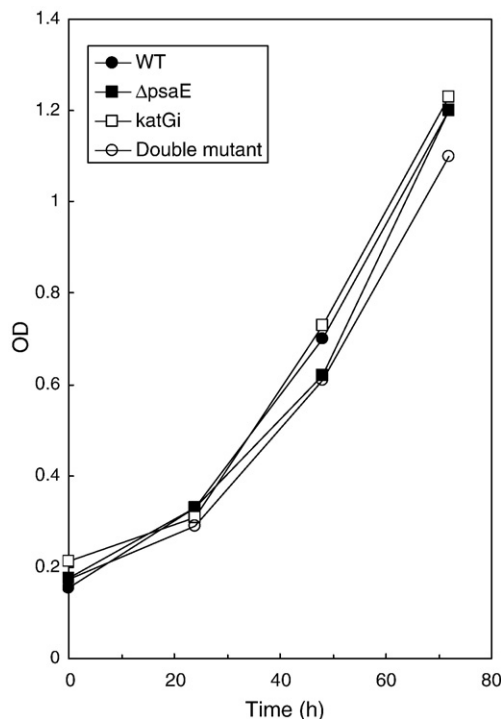


Fig. 7. Growth curves of WT *Synechocystis* sp. PCC 6803 and the $\Delta psaE$, *katGi* and $\Delta psaE$ –*katGi* mutants at $25 \mu mol$ photons $m^{-2} s^{-1}$. This experiment was repeated 3 times with similar results.

in WT cells. We conclude that the $\Delta psaE$ mutant produces more ROS during illumination than WT, but the increased activity of antioxidant enzymes, such as catalase and possibly SOD, efficiently scavenges the extra ROS formed in $\Delta psaE$.

3.4. Photosensitivity of a double mutant deficient in *PsaE* and in catalase

The compensatory up-regulation of protective mechanisms, e.g. catalase and SOD, could explain the low photosensitivity of the $\Delta psaE$ mutant reported in previous studies [21]. Therefore, we generated a catalase deleted mutant *katGi* and a double mutant $\Delta psaE$ –*katGi*. PCR and RT-PCR experiments show that they fully segregated (Fig. 5A). Accordingly, they displayed only a residual capacity to release oxygen from hydrogen peroxide (Fig. 4). This residual activity was previously reported in the *katGi* mutant by Tichy and Vermaas [26] who suggested that it could be due to peroxiredoxins. Several genes encoding those detoxifying enzymes are present in cyanobacteria [42–45]. Considering the essential role of the thioredoxin-dependent alkyl hydroperoxide-reductase AhpC, a member of the 2-Cys peroxiredoxin family, in the response of cyanobacteria to oxidative stress [44,46], we estimated the level of *ahpC* transcripts by RT-PCR. The transcripts were present in the *katGi* and $\Delta psaE$ –*katGi* mutants, but they were virtually undetectable in WT and in the

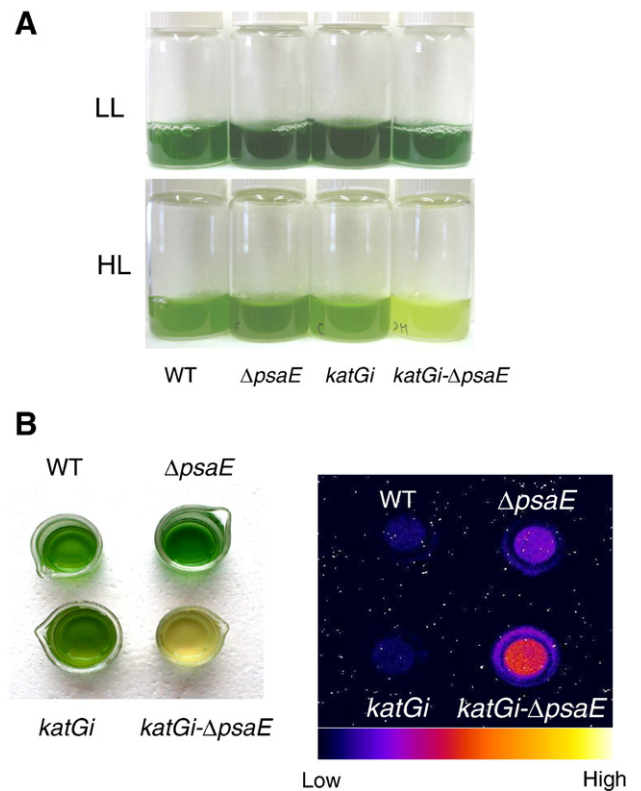


Fig. 8. Effects of high light stress ($500 \mu mol m^{-2} s^{-1}$ for 18 h) on *Synechocystis* sp. PCC 6803 (WT, $\Delta psaE$ single mutant, *katGi* single mutant and $\Delta psaE$ –*katGi* double mutant). A) Cell pigmentation. B) Intensity of lipid peroxidation measured by autoluminescence imaging. Acquisition time: 60 min. Randomly distributed white spots result from stray radiation in the range of gamma and cosmic rays.

ApsaE mutant (Fig. 5B). This finding suggests that peroxiredoxins could participate in the protection against H_2O_2 when catalases are missing.

As previously shown [26], mutational suppression of catalase does not significantly affect cell growth (Fig. 7). Similarly, growth of the *ApsaE*–*katGi* double mutant in low light ($\sim 25 \mu\text{mol m}^{-2} \text{s}^{-1}$) was close to that of WT and the single mutants. However, the double mutant behaved very differently from the other strains when PFD was increased. This is illustrated by the experiment shown in Fig. 8 where the WT, the double mutant *ApsaE*–*katGi* and the single mutants grown in low light were exposed to a high light treatment ($500 \mu\text{mol m}^{-2} \text{s}^{-1}$ for 18 h). Lipid peroxidation and oxidative stress were analyzed after light stress with a new imaging method based on spontaneous photon emission. This technique measures the faint light emitted spontaneously by living organisms and originating from $^1\text{O}_2$ and excited triplet state carbonyl groups [33,47], the byproducts of the slow spontaneous decomposition of lipid peroxides and endoperoxides [48,49]. In plants, the intensity of the imaged autoluminescence is well correlated with lipid peroxidation measured by biochemical assays [50,51]. The *ApsaE*–*katGi* double mutant bleached in high light (Fig. 7A) and exhibited a strong increase in autoluminescence (Fig. 7B), indicating oxidative stress and extensive lipid peroxidation. In contrast, WT and the single mutants remained green and showed a very low spontaneous luminescence, indicating that they are tolerant to photooxidative stress. The *ApsaE* mutant showed, however, a small increase in luminescence compared to WT and *katGi*, indicating that *ApsaE* has decreased capacity to tolerate photooxidative stress conditions than the latter strains. Clearly, the *ApsaE* mutant is sensitive to photooxidative stress and lipid peroxidation, especially when the catalase activity was inhibited by deletion of the *katG* gene.

4. Discussion

As previously reported [8,17], the absence of the PsaE subunit of PSI had no significant impact on photoautotrophic growth of *Synechocystis* cells. However, Thomas et al. [21] reported differences in the carotenoid composition between WT *Synechocystis* and the *ApsaE* mutant, which could be interpreted as a shift towards more oxidative growth conditions. From our photoacoustic and P700 redox state measurements, we can conclude that the change in carotenoid content was not due to a decrease in energy dissipation via cyclic electron flow. Actually, photochemical ES in far-red light in the *ApsaE* mutant was increased, rather than decreased, relative to WT. The extra ES was strictly dependent on the presence of oxygen, suggesting the occurrence of an electron transfer to oxygen in the mutant. It is possible that the absence of PsaE reduced the efficiency of electron flux to the PSI acceptors, favoring leakage of electrons to oxygen. Since photoacoustic measurements were performed at a low modulation frequency (16 Hz), the measured ES reflects photochemical products with a rather long lifetime, in the ms time range [34]. We do not know exactly the photochemical products responsible for the increased ES in *ApsaE*, but possible candidates could be long-lived molecules, such as e.g. ATP or H_2O_2 . The latter is the likely product of direct reduction of oxygen. For alternative pathways

involving sequential biochemical reactions, like photorespiration, detection by photoacoustic spectroscopy is hampered by strong damping of the modulation [34].

Oxygen photoreduction by the photosynthetic electron chain, also called Mehler reaction or water–water cycle, is present in all photosynthetic organisms [15], suggesting a physiological role for this reaction [52,53]. The Mehler reaction has been assumed to be a mechanism that dissipates excess light energy [54–56] and modulates state transitions [57]. A chronic oxygen-photoreduction activity in *Synechocystis* cells that lack the PsaE protein is further supported by the up-regulation of enzymatic systems that are involved in the detoxification of the byproducts of oxygen photoreduction, namely catalase and SOD. Furthermore, the increased activity of catalase was crucial for the survival of PsaE-deficient *Synechocystis* cells since blockage of this activity by sodium azide led to a stimulated production of ROS relative to WT and to growth impairment. When catalase was suppressed in *ApsaE* by mutation (double mutant *katGi*–*ApsaE*), a photosensitive phenotype was obtained. Consequently, our study indicates that one of the physiological functions of PsaE is to avoid unwanted leakage of electrons to oxygen which could lead to oxidative stress. It can be assumed that this function results from the optimization by PsaE of the interactions and electron transfers between PSI, ferredoxin and FNR. The main effect of *psaE* gene deletion in *Synechocystis* was reported to be on the dissociation of the PSI/ferredoxin complex [9]. Therefore, our results suggest that the decreased lifetime of this complex favors electron flow towards oxygen at the expense of NADP. Alternatively, PsaE could act as a shield limiting oxygen diffusion to and interaction with the PSI electron acceptors.

In the vascular plant *Arabidopsis thaliana*, elimination of the PsaE protein by disruption of the two *psaE* genes strongly affected growth rate, plant size and fertility [23]. In spite of this strong phenotype, the PsaE protein was regarded as dispensable due the possibility of photoautotrophic growth, although the mutant exhibited a high chlorophyll fluorescence and a high photosensitivity, suggesting that the photosynthetic electron transfer chain was perturbed. However, it is difficult to determine whether the photosynthetic changes in the *Arabidopsis psaE1 psaE2* double mutant are a direct consequence of the loss of the PsaE protein on photosynthesis or a secondary consequence due e.g. to chronic photooxidative stress. It is unfortunate that oxidative stress was not analyzed in the PsaE-deficient *Arabidopsis* plants. Nevertheless, the growth capacity of the cyanobacterial *ApsaE* mutant, close to that of WT, compared to the severe growth phenotype of the corresponding *Arabidopsis* mutant is puzzling.

Like cyanobacteria, plant chloroplasts contain ROS-scavenging enzymes (SOD, ascorbate peroxidase) which should have rescued the *Arabidopsis psaE* mutant, allowing normal growth rates and photosynthetic electron transport. A possible explanation for this difference between cyanobacteria and vascular plants might be that the intracellular oxygen concentration is probably higher in terrestrial organisms than in aquatic ones, according to the low solubility of oxygen in water (21% of oxygen in the atmosphere compared to $\sim 1\%$ of oxygen dissolved in water). Moreover, a true respiratory chain is present in the thylakoids of cyanobacteria [58,59] bearing a cytochrome *c*

oxidase whereas chlororespiration in chloroplasts is mediated by the plastid terminal oxidase PTOX [60]. The chlororespiratory electron flow catalyzed by PTOX is supposed to proceed at a very low rate [61]. Therefore, it is likely that the cyanobacterial cytochrome *c* oxidase and the plant PTOX do not have the same efficiency to maintain a relatively low oxygen concentration in the vicinity of the photosystems. It should also be mentioned that the genome of *Anabaena* contains not less than three genes encoding cytochrome *c* oxidase, two of them being transcribed depending of the nitrogen availability. Deletion of these two genes prevents cell growth in molecular nitrogen due to an excessive oxygen level in heterocysts leading to nitrogenase inactivation [62]. Therefore, because of this multiplicity of cyanobacterial oxidases and their marked effect on the cellular concentration of oxygen, limitation of electron transfer to oxygen at the PSI reducing side could be more crucial in vascular plants than in cyanobacteria.

According to Helman et al. [63], at least two flavoproteins would be involved in a Mehler-type reaction in *Synechocystis*, constituting a means of eliminating excess electrons in a controlled manner through a water–water cycle. Those flavoproteins have been identified in cyanobacteria and in primitive eukaryotic green algae, but similar sequences have not been found in the *Arabidopsis* genome. It is thus possible that electron transfer to oxygen mediated by these special flavoproteins will compete with the electron leakage to oxygen associated with the PsAE loss, and this could reduce the negative impact of the latter reaction in cyanobacteria compared to vascular plants. Considering the results reported here, it would be interesting to determine whether oxygen photoreduction is induced in the *Arabidopsis psaE1 psaE2* mutant.

To sum up, the presented results shed new light on the physiological and regulatory role of a PSI subunit. Although deletion of PsAE had little visible effect on photosynthesis of *Synechocystis* cells, a part of the photosynthetic electron flow was diverted towards oxygen causing a chronic formation of ROS at the PSI reducing side. In moderate light, *Synechocystis* cells are able to face this phenomenon by upregulating a range of detoxification systems including carotenoids [21], catalase and SOD (this study). However, when those systems are overwhelmed, e.g. in high light or when catalase activity is inhibited, PsAE-deficient cells can suffer ROS toxicity. Thus, although PsAE is not essential for *in vivo* linear and cyclic electron fluxes mediated by PSI, the presence of this PSI protein is required to limit oxygen reduction in the light and hence to prevent photooxidative damage.

Acknowledgements

We would like to thank Geneviève Guedeney (CEA/Cadarache, France) for the help in growing *Synechocystis* cells. The *AndhB* mutant was received from Prof. T. Ogawa.

References

- [1] J.H. Goldbeck, Structure and function of Photosystem I, *Ann. Rev. Plant Physiol. Mol. Biol.* 43 (1992) 293–324.
- [2] P.R. Chitnis, Photosystem I, *Plant Physiol.* 111 (1996) 661–669.
- [3] J. Barber, Photosystem II: an enzyme of global significance, *Biochem. Soc. Trans.* 34 (2006) 619–631.
- [4] T.S. Ambrust, P.R. Chitnis, J.A. Guikema, Organization of photosystem I polypeptides examined by chemical cross-linking, *Plant Physiol.* 111 (1996) 1307–1312.
- [5] C. Lelong, E.J. Boekema, J. Kruip, H. Bottin, M. Rögner, P. Sétif, Characterization of a redox active cross-linked complex between cyanobacterial photosystem I and soluble ferredoxine, *EMBO J.* 15 (1996) 2160–2168.
- [6] N. Weber, H. Strotmann, On the function of subunit PsAE in chloroplast photosystem I, *Biochim. Biophys. Acta* 1143 (1993) 204–210.
- [7] F. Rousseau, P. Sétif, B. Lagoutte, Evidence for the involvement of PSI-E subunit in the reduction of ferredoxin by photosystem I, *EMBO J.* 12 (1993) 1755–1765.
- [8] Q. Xu, Y. Jung, V.P. Chitnis, J.Z. Guikema, J.H. Goldbeck, P.R. Chitnis, Mutational analysis of photosystem I polypeptides in *Synechocystis* sp. PCC6803. Subunit requirements for reduction of NADP⁺ mediated by ferredoxin and flavodoxin, *J. Biol. Chem.* 269 (1994) 21512–21518.
- [9] P. Barth, B. Lagoutte, P. Sétif, Ferredoxin reduction by Photosystem I from *Synechocystis* sp. PCC 6803: toward an understanding of the respective role of subunits PsAD and PsAE in ferredoxin binding, *Biochemistry* 37 (1998) 16233–16241.
- [10] K. Meimberg, B. Lagoutte, H. Bottin, U. Mühlendorf, The *psaE* subunit is required for complex formation between Photosystem I and flavodoxin from the cyanobacterium *Synechocystis* sp. PCC 6803, *Biochemistry* 37 (1998) 9759–9767.
- [11] P. Jordan, P. Fromme, H.T. Witt, O. Klukas, W. Saenger, N. Krauss, Three-dimensional structure of cyanobacterial photosystem I at 2.5 Å resolution, *Nature* 411 (2001) 909–917.
- [12] H. Oh-Oka, Y. Takahashi, K. Kuriyama, K. Saeki, H. Matsubara, The protein responsible for center A/B in spinach photosystem I: isolation with iron–sulfur cluster(s) and complete sequence analysis, *J. Biochem.* 103 (1988) 962–968.
- [13] P.R. Chitnis, Q. Xu, V.P. Chitnis, R. Nechushtai, Function and organization of Photosystem I polypeptides, *Photosynth. Res.* 44 (1995) 23–40.
- [14] P. Sétif, N. Fischer, B. Lagoutte, H. Bottin, J.-D. Rochaix, The ferredoxin docking site of photosystem I, *Biochim. Biophys. Acta* 1555 (2002) 204–209.
- [15] K. Asada, The water–water cycle in chloroplasts: scavenging of active oxygens and dissipation of excess photons, *Annu. Rev. Plant Physiol. Mol. Biol.* 50 (1999) 601–639.
- [16] J.J. van Thor, H.T. Geerling, H.C.P. Matthijs, K.J. Hellingwerf, Kinetic evidence for the PsAE-dependent transient ternary complex photosystem I/ferredoxin/ferredoxin:NADP⁺ reductase in a cyanobacterium, *Biochemistry* 38 (1999) 12735–12746.
- [17] J. Zhao, W.B. Snyder, U. Mühlendorff, E. Rhiel, P.V. Warren, J.H. Golbeck, D.A. Bryant, Cloning and characterization of the *psaE* gene of the cyanobacterium *Synechococcus* sp. PCC 7002: characterization of a *psaE* mutant and overproduction of the protein in *Escherichia coli*, *Mol. Microbiol.* 9 (1993) 183–194.
- [18] N. Cassan, B. Lagoutte, P. Sétif, Ferredoxin–NADP⁺ reductase. Kinetics of electron transfer, transient intermediates, and catalytic activities studied by flash-absorption spectroscopy with isolated photosystem I and ferredoxin, *J. Biol. Chem.* 280 (2005) 25960–25972.
- [19] L. Yu, J. Zhao, U. Mühlendorff, D.A. Bryant, J.H. Golbeck, PsAE is required for *in vivo* cyclic electron flow around photosystem I in the cyanobacterium *Synechococcus* sp.7002, *Plant Physiol.* 103 (1993) 171–181.
- [20] D. Charlebois, D. Mauzerall, Energy storage and optical cross-section of PSI in the cyanobacterium *Synechococcus* PCC7002 and a *psaE*– mutant, *Photosynth. Res.* 59 (1999) 27–38.
- [21] D.J. Thomas, J. Thomas, P.A. Youderian, S.K. Herbert, Photoinhibition and light-induced cyclic electron transport in *ndhB*(–) and *psaE*(–) mutants of *Synechocystis* sp. PCC 6803, *Plant Cell Physiol.* 42 (2001) 803–812.
- [22] C. Varotto, P. Pesaresi, J. Meurer, R. Oelmüller, S. Steiner-Lange, F. Salamini, D. Leister, Disruption of the *Arabidopsis* photosystem I gene *psaE* affects photosynthesis and impairs growth, *Plant J.* 22 (2000) 115–124.

- [23] A. Ihnatowicz, P. Pesaresi, D. Leister, The E subunit of photosystem I is not essential for linear electron flow and photoautotrophic growth, *Planta* 226 (2007) 889–895.
- [24] R. Jeanjean, S. Bédou, M. Havaux, H.C.P. Matthijs, F. Joset, Salt-induced photosystem I cyclic electron transfer restores growth on low inorganic carbon in a type I NAD(P)H dehydrogenase deficient mutant of *Synechocystis* PCC6803, *FEMS Microbiol. Lett.* 167 (1998) 131–137.
- [25] I. Ardelean, H.C.P. Matthijs, M. Havaux, F. Joset, R. Jeanjean, Unexpected changes in Photosystem I function in a cytochrome C6-deficient mutant of the cyanobacterium *Synechocystis* PCC6803, *FEMS Microbiol. Lett.* 213 (2002) 113–119.
- [26] M. Tichy, W. Vermaas, In vivo role of catalase–peroxidase in *Synechocystis* sp. strain PCC 6803, *J. Bacteriol.* 181 (1999) 1875–1882.
- [27] C.K. Herbert, D.C. Fork, S. Malkin, Photoacoustic measurements *in vivo* of energy storage by cyclic electron flow in algae and higher plants, *Plant Physiol.* 94 (1990) 926–934.
- [28] J. Ravenel, G. Peltier, M. Havaux, The cyclic electron pathways around Photosystem I in *Chlamydomonas reinhardtii* as determined *in vivo* by photoacoustic measurement of energy storage, *Planta* 193 (1994) 251–259.
- [29] U. Schreiber, C. Klughammer, C. Neubauer, Measuring P700 absorbance changes around 830 nm with a new type of pulse modulation system, *Z. Naturforsch.* 43C (1998) 686–698.
- [30] P.C. Maxwell, J. Biggins, Role of cyclic electron transport in photosynthesis as measured by the photoinduced turnover of P700 *in vivo*, *Biochemistry* 15 (1976) 3975–3981.
- [31] Jakopitsch, G. Regelsberger, P.G. Furtmüller, F. Rüker, G.A. Peschek, C. Obinger, Catalase–peroxidase from *Synechocystis* is capable of chlorination and bromination reactions, *Biochem. Biophys. Res. Commun.* 287 (2001) 682–687.
- [32] A. Latifi, R. Jeanjean, S. Lemeille, M. Havaux, C.-C. Zhang, Iron starvation leads to oxidative stress in *Anabaena* sp. strain PCC 7120, *J. Bacteriol.* 187 (2005) 6596–6598.
- [33] M. Havaux, C. Triantaphylides, B. Genty, Autoluminescence imaging: a non-invasive tool for mapping oxidative stress, *Trends Plant Sci.* 11 (2006) 480–484.
- [34] S. Malkin, O. Canaani, The use and characteristics of the photoacoustic method in the study of photosynthesis, *Ann. Rev. Plant Physiol. Plant Mol. Biol.* 45 (1994) 493–552.
- [35] S. Malkin, N. Lasser-Ross, G. Bults, D. Cahen, Photoacoustic spectroscopy in photosynthesis, in: G. Akoyunoglou (Ed.), *Photosynthesis III. Structure and Molecular Organisation of the Photosynthetic Apparatus*, Balaban International Science Services, Philadelphia, 1981, pp. 1031–1042.
- [36] F.A.L.J. Peters, R. Van Spanning, R. Kraayenhof, Studies on well coupled Photosystem I-enriched subchloroplast vesicles. Optimization of ferredoxin-mediated cyclic photophosphorylation and electric potential generation, *Biochim. Biophys. Acta* 724 (1983) 159–165.
- [37] H. Mi, T. Endo, U. Schreiber, T. Ogawa, K. Asada, Electron donation from cyclic and respiratory flows to the photosynthetic intersystem chain is mediated by pyridine-nucleotide dehydrogenase in the cyanobacterium *Synechocystis* PCC-6803, *Plant Cell Physiol.* 33 (1992) 1233–1237.
- [38] N. Yermenko, R. Jeanjean, P. Prommeenate, V. Krasikov, P.J. Nixon, W.F. Vermaas, M. Havaux, H.C.P. Matthijs, Open reading frame *ssr2016* is required for antimycin A-sensitive photosystemI-driven cyclic electron flow in the cyanobacterium *Synechocystis* sp. PCC 6803, *Plant Cell Physiol.* 46 (2005) 1433–1436.
- [39] J.A. Imlay, Pathways of oxidative damage, *Annu. Rev. Microbiol.* 57 (2003) 395–418.
- [40] G. Forti, P. Gerola, Inhibition of photosynthesis by azide and cyanide and the role of oxygen in photosynthesis, *Plant Physiol.* 59 (1997) 859–862.
- [41] M. Havaux, G. Guedeney, M. Hagemann, N. Yermenko, H.C.P. Matthijs, R. Jeanjean, The chlorophyll-binding protein *IsiA* is inducible by high light and protects the cyanobacterium *Synechocystis* PCC6803 from photooxidative stress, *FEBS Lett.* 579 (2005) 2289–2293.
- [42] C. Obinger, G. Regelsberger, P.G. Furtmüller, C. Jakopitsch, F. Rüker, A. Pircher, G.A. Peschek, Catalase–peroxidases in cyanobacteria—similarities and differences to ascorbate peroxidases, *Free Rad. Res.* S2 (1999) 43–49.
- [43] M. Kobayashi, T. Ishizuka, M. Katayama, M. Kanehisa, M. Bhattacharyya-Pakrasi, H.B. Pakrasi, M. Ikeuchi, Response to oxidative stress involves a novel peroxiredoxin gene in the unicellular cyanobacterium *Synechocystis* sp. PCC 6803, *Plant Cell Physiol.* 45 (2004) 290–299.
- [44] N. Hosoya-Matsuda, K. Motohashi, H. Yoshimura, A. Nozaki, K. Inoue, M. Ohmori, T. Hisabori, Anti-oxidative stress system in cyanobacteria. Significance of type II peroxiredoxin and the role of 1-cys peroxiredoxin in *Synechocystis* sp. strain PCC 6803, *J. Biol. Chem.* 280 (2005) 840–846.
- [45] A. Latifi, M. Ruiz, R. Jeanjean, C.C. Zhang, PrxQ-A, a member of the peroxiredoxin Q family, plays a major role in defense against oxidative stress in the cyanobacterium *Anabaena* sp. strain PCC7120, *Free Radic. Biol. Med.* 42 (2007) 424–431.
- [46] H. Li, A. Singh, L.M. McIntyre, L.A. Sherman, Differential gene expression in response to hydrogen peroxide and the putative PerR regulon of *Synechocystis* sp. Strain PCC 6803, *J. Bacteriol.* 186 (2004) 3331–3345.
- [47] M. Flor-Henry, T.C. McCabe, G.L. de Bruxelles, M.R. Roberts, Use of a highly sensitive two-dimensional luminescence imaging system to monitor endogenous bioluminescence in plant leaves, *BMC Plant Biol.* 4 (2004) 19.
- [48] J.M. Gutteridge, B. Halliwell, The measurement and mechanism of lipid peroxidation in biological systems, *Trends Biochem. Sci.* 15 (1990) 129–135.
- [49] D. Vavilin, J.M. Ducruet, The origin of 115–130 °C thermoluminescence band in chlorophyll containing material, *Photochem. Photobiol.* 68 (1998) 191–198.
- [50] M.P. Johnson, M. Havaux, C. Triantaphylides, B. Ksas, A.A. Pascal, B. Robert, P.A. Davison, A.V. Ruban, P. Horton, Elevated zeaxanthin bound to oligomeric LHCII enhances the resistance of *Arabidopsis* to photo-oxidative stress by a lipid-protective, antioxidant mechanism, *J. Biol. Chem.* 282 (2007) 22605–22618.
- [51] M. Havaux, L. Dall'Osto, R. Bassi, Zeaxanthin has enhanced antioxidant capacity with respect to all other xanthophylls in *Arabidopsis* leaves and functions independent of binding to PSII antennae, *Plant Physiol.* 145 (2007) 1506–1520.
- [52] D.R. Ort, N.R. Baker, A photoprotective role for O₂ as an alternative electron sink in photosynthesis? *Curr. Opin. Plant Biol.* 5 (2002) 193–198.
- [53] A. Makino, C. Miyake, A. Yokota, Physiological functions of the water–water cycle (Mehler reaction) and the cyclic electron flow around PSI in rice leaves, *Plant Cell Physiol.* 43 (2002) 1017–1026.
- [54] K. Biehler, H. Fock, Evidence for the contribution of the Mehler-peroxidase reaction in dissipating excess electrons in drought-stressed wheat, *Plant Physiol.* 112 (1996) 265–272.
- [55] U. Heber, Irrungen, Wurrungen? The Mehler reaction in relation to cyclic electron transport in C3 plants, *Photosynth. Res.* 73 (2002) 223–231.
- [56] L. Rizhsky, H. Liang, R. Mittler, The water–water cycle is essential for chloroplast protection in the absence of stress, *J. Biol. Chem.* 278 (2003) 38921–38925.
- [57] G. Forti, G. Caldiroli, State transitions in *Chlamydomonas reinhardtii*. The role of the Mehler reaction in state 2-to-state 1 transition, *Plant Physiol.* 137 (2005) 492–499.
- [58] C.A. Howitt, W.F. Vermaas, Quinol and cytochrome oxidases in the cyanobacterium *Synechocystis* sp. PCC 6803, *Biochemistry* 37 (1998) 17944–17951.
- [59] G.A. Peschek, C. Obinger, M. Paumann, The respiratory chain of blue-green algae (cyanobacteria), *Physiol. Plant.* 120 (2004) 358–369.
- [60] D. Rumeau, G. Peltier, L. Courmac, Chlororespiration and cyclic electron flow around PSI during photosynthesis and plant stress response, *Plant Cell Environ.* 30 (2007) 1041–1051.
- [61] T. Joet, B. Genty, E.M. Josse, M. Kuntz, L. Courmac, G. Peltier, Involvement of a plastid terminal oxidase in plastoquinone oxidation as evidenced by expression of the *Arabidopsis thaliana* enzyme in tobacco, *J. Biol. Chem.* 277 (2002) 31623–31630.
- [62] A. Valladares, A. Herrero, D. Pils, G. Schmetterer, E. Flores, Cytochrome *c* oxidase genes required for nitrogenase activity and diazotrophic growth in *Anabaena* sp. PCC 7120, *Mol. Microbiol.* 47 (2003) 1239–1249.
- [63] Y. Helman, D. Tchernov, L. Reinhold, M. Shibata, T. Ogawa, R. Schwarz, I. Ohad, A. Kaplan, Genes encoding A-type flavoproteins are essential for photoreduction of O₂ in cyanobacteria, *Curr. Biol.* 13 (2003) 230–235.